

BBA 47697

## LOCALIZATION AND CHARACTERIZATION OF CYTOCHROMES FROM MEMBRANE VESICLES OF *ESCHERICHIA COLI* K-12 GROWN IN ANAEROBIOSIS WITH NITRATE

JOSÉ A. SÁNCHEZ CRISPÍN, MICHEL DUBOURDIEU and MARC CHIPPAUX \*

*Grupo de Biología Experimental, Facultad de Ciencias, Universidad de los Andes, Apartado Postal 281, Mérida (Venezuela)*

(Received December 5th, 1978)

**Key words:** Cytochrome *b*; Nitrate reductase; Anaerobiosis; Electron transport; Membrane vesicle; (*Escherichia coli*)

### Summary

Cytochromes *b* of anaerobically nitrate-grown *Escherichia coli* cells are analysed. Ascorbate phenazine methosulfate distinguishes low and high potential cytochromes *b*. Reduction kinetics performed at 559 nm presents a very complex pattern which can be analysed assuming that at least four *b*-type cytochromes are present. The electron transport chain from formate to oxygen would contain a low potential cytochrome *b*-556, a cytochrome *b*-558 associated to the oxidase, and a cytochrome *d* as the principal oxidase. Cytochrome *o* is also present, but seems to be functional only at low oxygen concentrations. A cytochrome *b*-556 associated to nitrate reductase is shown to belong to a branch of the formate-oxidase chain.

2-*N*-Heptyl-4-hydroxyquinoline-*N*-oxide affects the reduction kinetics in a very complex way. One inhibition site is in evidence between cytochrome *b*-558 and cytochrome *d*; another between the cytochrome associated to nitrate reductase and the nitrate reductase. A third inhibition site is located in the common part of the formate-nitrate and the formate-oxidase systems.

Ascorbate phenazine methosulfate is shown to donate electrons near cytochrome *b*-558.

---

\* Present address: Laboratoire de Chimie Bactérienne, CNRS, 31 Chemin Joseph Aiguier, 13274 Marseille, France.

Abbreviation: HQNO, 2-*n*-heptyl-4-hydroxyquinoline-*N*-oxide.

## Introduction

One of the first reports about nitrate reduction electron transport chain mentioned only one cytochrome *b* [1]. Later, Ruiz-Herrera and De Moss [2] revealed two *b*-type cytochromes, *b*<sub>I</sub> and *b*<sub>II</sub>, in this system. Their characteristics are rather similar and inhibit their differentiation. Recently, Enoch and Lester [3], purified both formate dehydrogenase and nitrate reductase, each one associated with an apparently specific cytochrome *b*. This confirms the existence of at least two cytochromes *b* in the chain formate-nitrate reductase. In this paper we show that the formate-nitrate electron transport chain is only part of a more complex electron transport system in which at least another dehydrogenase, NADH dehydrogenase and another acceptor, oxygen, are implicated. A more complete analysis of cytochrome *b* content in membrane vesicles of anaerobically nitrate-grown *Escherichia coli* cells is presented.

## Materials and Methods

*E. coli* Hfr P<sub>4</sub>X, 303 in Puig's collection is *Met*<sup>-</sup>, a gift from Dr. Wollman, Institut Pasteur, Paris.

The minimal medium is phosphate buffer (0.06 M, pH 8.0) with 0.4 g/l of ammonium chloride, 0.4 g/l MgSO<sub>4</sub> · 7H<sub>2</sub>O, with traces of iron and calcium. The growth medium is obtained by adding 1 g/l of bacto-peptone, 0.5 g/l of meat extract, and 0.5 g/l of yeast extract to the base medium. Glucose (2 g/l), potassium nitrate (1 g/l) and azide (0.1 mM), previously sterilized, are added to the complex medium just before inoculation. The inoculum is an anaerobic exponentially growing cell culture amounting to about 10% of the final volume.

The cells are grown anaerobically at 37°C and collected by centrifuging 1 h before the beginning of the stationary phase. The cells are washed three times with Tris-HCl buffer (0.01 M, pH 7.3) to eliminate nitrite and azide.

In such conditions the growth yield is about 2–3 g of wet cells/l. The cells are stored overnight at 5°C to prevent lysis, and then used to prepare the membrane vesicles.

Vesicles are prepared by a modification of the method of Corao et al. [4]. 100 g of wet cells are resuspended in 4 l of a buffer (0.03 M Tris-HCl, pH 8.0) containing 0.1% EDTA and 20% saccharose and maintained at 25°C, timing 15 min, under constant stirring. Then, lysozyme (10 mg/g of wet cells) is added. The incubation is stopped when approximately 90% of the cells have been transformed into spheroplasts. A phase contrast microscope is used for this determination. Spheroplasts are collected by centrifugating at 10 000 × *g* for 30 min, resuspended and incubated in the same volume of 0.02 M Tris-HCl (pH 7.5), containing DNAase and RNAase (0.2 and 0.1 mg/g of wet cells, respectively). When the lysis is estimated to be more than 95% and the viscosity has almost disappeared, the suspension is centrifuged at 5000 × *g* for 10 min to eliminate whole cells, unlysed spheroplasts and cell wall residues.

The vesicles are centrifuged at 30 000 × *g* for 30 min and washed three times with 0.02 M Tris-HCl (pH 7.5). The last washing buffer contains 0.1 mM MgCl<sub>2</sub>.

The vesicular pellet is then divided into 1 g fractions and stored at -20°C.

Membrane vesicles can be stored for at least six months under these conditions without losing respiratory activity. Before use, they are resuspended into a 0.06 M phosphate buffer (pH 7.3), containing 0.1 mM  $\text{MgCl}_2$ . The suspension is homogenized by a 2 s sonication.

Cytochrome reduction kinetics were performed in two types of spectrophotometers. A Cary-14 equipped with a 0–0.1 full scale potentiometer was used to perform preliminary experiments. Kinetics were obtained by recording first at 559 nm and then at 575 nm, and graphically adding the two curves. In general an increase of the baseline was observed during the reduction process, except when using ascorbate-reduced phenazine methosulfate as an electron donor. All experiments presented in this work were repeated in an Aminco double-wavelength spectrophotometer. Low temperature spectra were recorded with the liquid nitrogen attachment of the Aminco apparatus.

In general cytochrome reduction kinetics were performed in the presence of an initial oxygen concentration of 240  $\mu\text{M}$ . This is the oxygen concentration present in a neutral buffer exposed to air at 25°C. Oxygen uptake was followed in an oxygraph apparatus equipped with a recording attachment. Temperature was maintained at 25°C. Cytochromes *b* will be characterized by their  $\alpha$  band maximum in nm at liquid nitrogen temperature.

Ultraviolet light (360 nm) irradiation experiments were performed at 4°C in a closed system to prevent evaporation. The vesicular membrane suspension was about 3 mm thick. A Mineralight lamp was placed at 15 nm above the suspension at a temperature of 4°C. At different times, aliquots were taken and tested for cytochrome reduction.

Proteins were determined according to Lowry et al. [5].

## Results

### *Maximum levels of cytochrome b reduction in the presence of several donors*

Maximum cytochrome *b* reduction levels measured in the  $\alpha$  band are shown in Table I. Dithionite is considered to reduce the totality of *b*-type cytochromes and is used to determine 100% level of reduction. Formate and NADH reduce 95% of the cytochrome content while ascorbate phenazine methosulfate reduces only 58% of it.

The reduction level of cytochrome *b* obtained in the presence of formate alone does not change if NADH or ascorbate phenazine methosulfate is added. Addition of formate or NADH to the ascorbate phenazine methosulfate-reduced system produces the reduction obtained with formate or NADH alone.

An ascorbate phenazine methosulfate concentration increase does not modify the cytochrome *b* reduction level. Two groups of cytochromes are then differentiated. The first one, not reduced by ascorbate phenazine methosulfate, is characterized by an  $\alpha$  band at 558 nm in our spectrophotometer (Fig. 1). The second group, ascorbate phenazine methosulfate reduced, presents an  $\alpha$  band at 559 nm. The same difference can be registered at liquid nitrogen temperature; although, the dithionite-reduced system exhibits only one absorption band under these conditions. Fig. 1 represents the average of numerous and reproducible experiments.

High NADH concentration ( $5 \cdot 10^{-3}$  M) produces (Table I) a reduction

TABLE I

LEVELS OF CYTOCHROME *b* REDUCTION BY SEVERAL ELECTRON DONORS. EFFECT OF CO ON THESE LEVELS

The sample cell (2.5 ml) contains the reduced system while the reference cell contains the same amount of air-oxidized vesicles. Levels of cytochrome reduction are calculated from the absorption difference between 559 nm and 575 nm at room temperature. Results are expressed in percent of the maximum reduction level obtained with dithionite (0.5 nmol of reduced cytochrome *b*/mg of proteins using a molar extinction coefficient of  $17.5 \text{ nM}^{-1} \cdot \text{cm}^{-1}$  [6]. All systems contain 1.25 mg of protein/ml. Donor concentrations are  $2 \cdot 10^{-3} \text{ M}$  for NADH and formate (when not otherwise indicated),  $2 \cdot 10^{-2} \text{ M}$  for ascorbate and  $10^{-4} \text{ M}$  for phenazine methosulfate (PMS). Pure CO, when used, was bubbled for 3 min.

Electron donor	Reduced against oxidized (%)	Reduced + CO against oxidized (%)	Reduced against reduced + CO (%)
Dithionite	100	90	10
Formate	96	86	10
Formate + NADH	96	—	—
NADH ( $5 \cdot 10^{-3} \text{ M}$ )	95	82	12
NADH ( $10^{-4} \text{ M}$ )	85	—	—
PMS	58	46	8
PMS + formate + ascorbate	96	—	—
Ascorbate	2	—	—

similar to that produced by formate. An NADH concentration of around  $10^{-4} \text{ M}$  allows about a 85% cytochrome *b* reduction level. Keeping in mind that the electron donor is added to the oxygen-containing system, this phenomenon can be attributed to the difference in the redox potential values between formate ( $-420 \text{ mV}$  for formate/ $\text{CO}_2$ ) and NADH ( $-320 \text{ mV}$  for NADH/NAD) which

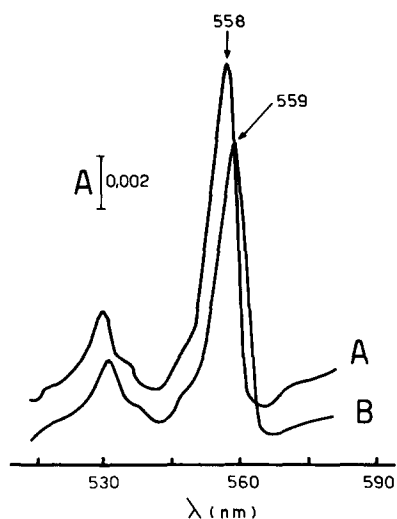


Fig. 1. (A) The differential spectrum between cytochromes *b* reduced by formate (sample) and cytochromes *b* reduced by ascorbate phenazine methosulfate. (B) The spectrum of cytochromes *b* reduced by ascorbate phenazine methosulfate. The reference cell contains air-oxidized vesicles. In each case the spectrum is recorded when reduction of cytochromes *b* is completed. Vesicles 0.6 mg of protein/ml; formate  $5 \cdot 10^{-3} \text{ M}$ . Ascorbate phenazine methosulfate: ascorbate  $2 \cdot 10^{-2} \text{ M}$ ; phenazine methosulfate  $10^{-4} \text{ M}$ . Temperature  $25^\circ \text{C}$ .

shows the presence of a very electronegative *b*-type cytochrome. A preliminary potentiometric study gives a value of approximately  $-250$  mV for the redox potential of cytochrome *b*. Deeb and Hager [7] have already described a very negative potential form of their purified cytochrome *b*. Such a low potential electron carrier would not be reduced by ascorbate phenazine methosulfate.

Differential spectra between reduced vesicles with and without CO bubbling made evident that all donors can reduce the same amount of CO-binding cytochrome, which represents about 10% of the total absorption of cytochrome *b* (Table I). The  $\alpha$  band of this cytochrome is centered at 559 nm in our spectrophotometer, and could correspond to the cytochrome *o* already described by Castor and Chance [8].

All the donors we have used can reduce a cytochrome *d* characterized by a reduced versus oxidized absorption peak at 634 nm.

#### *Cytochrome b reduction level during steady states*

Both nitrate and oxygen can reoxidize completely the cytochromes *b* reduced by NADH and formate if sufficient concentration of the acceptor is used. It shows that part of the respiratory chain is common to nitrate and oxygen-reducing systems.

The reduction level of cytochrome *b* obtained during the steady state is about 50% with molecular oxygen and only 2–3% with nitrate (Table II). This difference agrees with the higher electron transfer capacity of the nitrate-specific chain. It is surprising the way in which the steady state obtained in the presence of formate (or NADH) and oxygen affects the level of reduced cytochrome *b*. In effect, if oxygen is added after formate, 65% of the cytochrome reduction level is reached in the steady state, but this level is only about 25% if formate is added after oxygen. An explanation of this phenomenon will be given later in this paper.

CO bubbling can completely prevent cytochrome *b* reoxidation. This discards the possibility of autooxydizable cytochromes *b* in the chain. On the other

TABLE II

LEVELS OF STEADY-STATE CYTOCHROME *b* REDUCTION IN THE PRESENCE OF SEVERAL ELECTRON DONORS AND ACCEPTORS

Conditions are identical to those of Table I. When oxygen is added before the donor, the donor is added to an air-saturated vesicle suspension (oxygen concentration,  $240 \mu\text{M}$ ). When the acceptor is added after the electron donor, cytochrome *b* were first completely reduced with the donor; in such a case  $\text{O}_2$  is  $40 \mu\text{M}$  and  $\text{NO}_3^-$  is  $10^{-2}$  M. The results are expressed in percent of maximum reduction level obtained with each substrate.

Donor	Acceptor		
	Nitrate % (reduced)	Oxygen	
		Added after donor (% reduced)	Added before donor (% reduced)
Formate	2	64	25
NADH	2	53	17
PMS	3	40	32
Ascorbate	100	100	—

hand, azide can prevent any reoxidation of the chain in the presence of nitrate. The very small cytochrome *b* reduction level obtained with ascorbate does not change upon addition of  $\text{NO}_3^-$  or  $\text{O}_2$ . It is in agreement with the absence of ascorbate nitrate reductase or ascorbate oxidase activity observed with these membrane vesicles.

*Kinetics of cytochrome *b* reduction in the presence of formate and an initial oxygen concentration*

Fig. 2 shows the simultaneous reductions of cytochromes *b* and *d* and the process of oxygen consumption. At zero time the system contains  $240\ \mu\text{M}$  of dissolved oxygen. The cytochrome *b* reduction curve is divided into four phases. Phase I corresponds to a pseudo steady state in the course of which oxygen is consumed at the expense of formate. We call it 'pseudo steady' since it does not correspond to the steady state obtained upon  $\text{O}_2$  reoxidation of

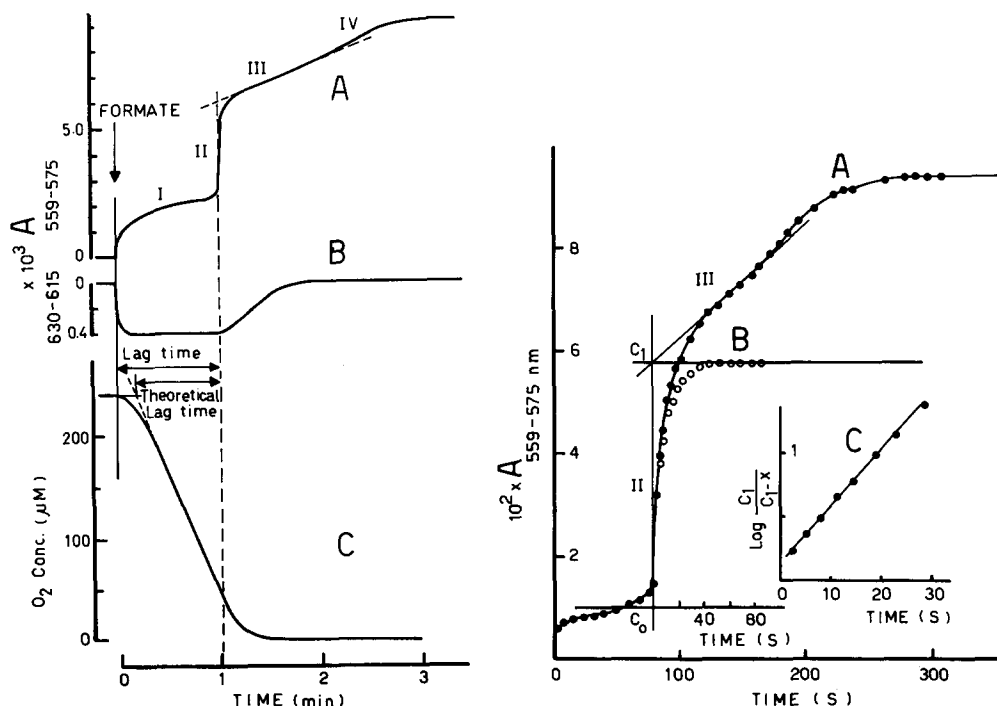


Fig. 2. Simultaneous recording of cytochromes *b* (curve A) and *d* (curve B) reduction and oxygen uptake (curve C). At zero time the concentration of dissolved oxygen is  $240\ \mu\text{M}$ . The reaction is started by formate addition. Vesicles  $1.2\ \text{mg}$  of proteins/ml; formate  $5 \cdot 10^{-3}\ \text{M}$ . Temperature  $25^\circ\text{C}$ . Lag time is defined as the time elapsed between electron donor addition and the starting of phase II.

Fig. 3. Graphical decomposition of phases II and III. (A) The cytochromes *b* reduction curve (see Fig. 2A). The beginning of phase II is taken as zero time and the reduction level at this point is  $C_0$ . The phase III slope is extrapolated to this new zero time (point  $C_1$ ).  $C_1 - C_0$  corresponds to the reduction of cytochrome *b* during phase II. The extrapolated line corresponding to phase III is subtracted from curve A and gives curve B which represents phase II. Curve C shows that curve B can be considered to be first-order kinetics. Vesicles:  $10\ \text{mg/ml}$ ; donor: formate  $5 \cdot 10^{-3}\ \text{M}$ . Temperature  $25^\circ\text{C}$ . A Cary 14 spectrophotometer was used.

reduced vesicles. The reduced cytochrome *b* level is not constant but increases slightly during this phase.

In phase II a very rapid reduction occurs as the system approaches anaerobiosis, while the dissolved oxygen concentration is about 40  $\mu\text{M}$  and cytochrome *d* begins to be reduced (Fig. 2B). This shows that the oxygen concentration is beginning to act as a limiting factor and that the cytochrome *d* appears as the operative oxidase. Whereas phase II starts simultaneously with cytochrome *d* reduction, it terminates much more rapidly than does the reduction of cytochrome *d*. At the end of phase II the concentration of oxygen is still in the order of 30  $\mu\text{M}$ . Thus, phase II apparently does not depend directly on the oxygen decrease.

The point at which cytochrome *b* reduction kinetics has been divided into phases III and IV corresponds to a slope increase, which indicates that these phases cannot be attributed to the same reduction process. The transition between phase III and phase IV coincides with the completion of the cytochrome *d* reduction. At this point our oxygraph does not register any dissolved oxygen (less than or equal to 1  $\mu\text{M}$ ).

Phase IV, which occurs only when conditions are anaerobic or very close to an anaerobic state, must correspond to the reduction of a cytochrome having a great affinity towards oxygen.

#### *Graphical analysis of phases II and III*

While a slope increase between phases III and IV justifies the division into these two phases, the distinction of phases II and III should be discussed. Our argument is empirical and is based on the following premise. In a linear respiratory chain, while the electron acceptor is consuming up, the reduction of intermediary compounds (cytochrome *b*) will be a sigmoidal curve almost parallel with terminal oxidase reduction (cytochrome *d*). Electron carriers, which are not located in the main chain but in a branch, without electron escape, may follow a first-order rate curve with respect to the concentration of the oxidized form.

If the linear part of phase III is extrapolated to the origin of phase II and graphically subtracted from this rapid phase (Fig. 3), the resulting phase II appears as a first-order kinetics (insert of Fig. 3). It is apparently the only way to get a simple-order kinetics from such rapid reduction. The rapid reduction would then reflect the superposition of two simultaneous reduction processes: one of them of apparent first order, independent of the oxygen uptake rate ( $k = 0.3\text{--}0.4\text{ s}^{-1}$ ), and the other sigmoidal, parallel to cytochrome *d* reduction.

It seems reasonable to conclude that phase II cytochrome *b* is not located in the main formate-oxygen chain but rather in a branch of the system.

#### *Effect of initial oxygen concentration on cytochrome b reduction of phase II*

Fig. 4A and B show that phase II starts at a residual oxygen concentration of 40–42  $\mu\text{M}$  when the initial concentration is at least 80–90  $\mu\text{M}$ . For initial values below 80  $\mu\text{M}$ , phase II starts at residual oxygen concentrations smaller than 40  $\mu\text{M}$ . It means that oxygen is already limiting when oxygen concentration is 80  $\mu\text{M}$ . We could determine a Michaelis constant of 32  $\mu\text{M}$  oxygen for the oxidase of our system. From the results described in Fig. 2, it is reasonable

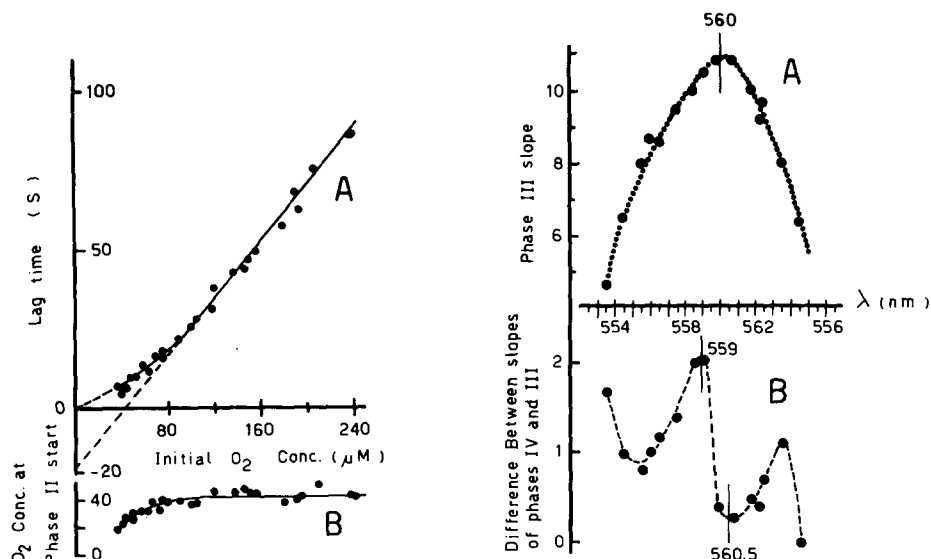


Fig. 4. Effect of initial  $O_2$  concentration upon the beginning of phase II. Each experiment, which corresponds to a different initial  $O_2$  concentration obtained by argon bubbling, involves: (1) an oxygen uptake recording, and (2) a 559–575 nm absorption recording. Both determinations are performed simultaneously. Lag time is determined from the spectrophotometer recorder, and reported on the oxygen record. At this point the  $O_2$  concentration is read. Theoretical lag time is defined in Fig. 2C. Curves A and B, respectively, represent theoretical lag time and oxygen concentration at the beginning of phase II as a function of the initial oxygen concentration. Vesicles: 0.8 mg of protein/ml; formate:  $2 \cdot 10^{-3}$  M. Temperature:  $25^\circ\text{C}$ .

Fig. 5. Action spectra of cytochromes *b* of phases III and IV. Cytochromes *b* reduction kinetics (see Fig. 2) is recorded at different wavelengths (2–3 times for each wavelength value) with as many controls at 559 nm. The slopes of the linear part of phases III and IV are measured. Curve A represents the slope of phase III as a function of the wavelength, whereas curve B represents the difference between the slopes of phases IV and III as a function of the wavelength. Vesicles: 1 mg of protein/ml. Formate:  $5 \cdot 10^{-3}$  M. Temperature:  $25^\circ\text{C}$ .

to attribute this  $K_m$  to cytochrome *d*. It follows that the reduction of the cytochrome *b* which is located in the ramification of the formate-oxygen pathway, cannot occur during the steady state. It seems to need a higher energy state of the chain, attained with a small decrease of oxidase activity.

The instantaneous start of phase II upon short CO bubbling appears to support this conclusion (Fig. 6). The kinetics rapidly reaches a steady-state level corresponding to 70% of reduced cytochromes, similar to the level obtained upon oxygen addition to reduced vesicles (Table II).

These results confirm the existence of two types of steady-state levels (25–30% and 65–70%) which differ by a value corresponding to the cytochrome *b* reduction of phase II. It has not been possible to obtain intermediary levels of steady states by very slight CO inhibition, which is the expected result for a cytochrome *b* not located in the direct pathway.

Phase III is always parallel to cytochrome *d* reduction and reveals the existence of cytochrome(s) *b* located in the main chain (formate dehydrogenase-oxidase). The linear part of phase IV cannot correspond to an intermediate, but rather to a terminal oxidase. It could be tentatively attributed to



cytochrome *o*, since reduction begins at oxygen concentrations smaller than 1–2  $\mu\text{M}$ . At such low oxygen concentrations cytochrome *d* can be considered reduced. This implies the existence of two oxidases. The first, cytochrome *d*, would be characterized by a high activity and low affinity towards oxygen. The second, cytochrome *o*, would present a quite strong affinity towards oxygen but would contribute very little to oxygen consumption.

*Spectral characterization of the different phases of the cytochrome b reduction curve*

Phases I and II were characterized spectrophotometrically at liquid nitrogen temperature by freezing the reaction mixture at different times after formate addition. The  $\alpha$  band absorption maxima of phases I and II are not identical (556.5 nm and 556 nm, respectively). Although the difference is very small, it is reproducible. The value of 556 nm makes possible the identification of phase II with the reduction of nitrate reductase-associated cytochrome *b* [3].

The steady-state (phase I) absorption maximum (556.5 nm) must be due mostly to the low potential formate dehydrogenase-associated cytochrome *b*, since it is the first cytochrome of the formate- $\text{O}_2$  chain. A small contribution must be expected from the other cytochromes *b* of the main chain, in particular from the cytochrome which is associated to the oxidase.

Phases III and IV were characterized by their action spectra recording the cytochrome *b* reduction curves at several wavelengths. The slope of phase III is maximum at 560 nm (Fig. 5). This phase may correspond to the already described cytochrome *b*-558 located near the terminal cytochrome *d* [9,10].

Phase IV was characterized by plotting the difference between the slopes of phase IV and III. Fig. 5 indicates the different nature of cytochromes *b* reduced in the course of phase III and IV. The negative spectrum (560.5 nm) corresponds to phase III (cytochrome *b*-558), whereas phase IV is characterized by a positive absorption maximum at 559 nm. This agrees with our hypothesis, which associates the later phase with cytochrome *o* reduction.

*The effects of HQNO inhibition on cytochrome b reduction by formate and its reoxidation by  $\text{O}_2$  and  $\text{NO}_3^-$*

The cytochrome *b* reduction curve in presence of HQNO is shown in Fig. 6A. The inhibition produces a significant increase in the steady-state level (60% under these conditions). Liquid nitrogen temperature spectra do not reveal differences between the two phases of the reduction curve.

The steady-state cytochrome *b* reduction level would be principally due to the low potential cytochrome, since the addition of ascorbate phenazine methosulfate produces an almost instantaneous reduction of the rest of cytochrome *b* (Fig. 6). This result, consistent with an inhibition site located at the electron-donating side of the low potential cytochrome *b*, is supported by the fact that  $\text{NO}_3^-$  is unable to produce any reoxidation in the steady state of the HQNO-treated system.

Oxygen addition to the fully reduced system does not produce any more reoxidation of cytochrome *b* (Fig. 6). This implies the existence of an inhibition site between cytochrome *b* near the oxidase and the terminal oxidase.

Without HQNO cytochrome *b* reoxidation by  $\text{NO}_3^-$  cannot be registered

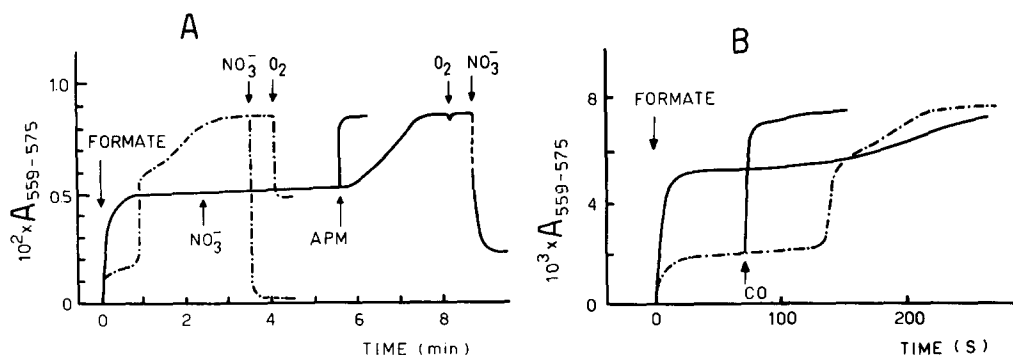


Fig. 6. Effect of HQNO and CO on the cytochrome *b* reduction kinetics by formate. Experimental conditions are the same as in Fig. 2A except for inhibitor additions. (A) HQNO (130  $\mu$ M) is added 5 min before formate (—). ·····, control without HQNO. Oxygen is added as a 100  $\mu$ l aliquot of an oxygen-saturated buffer (final concentration about 40  $\mu$ M). Nitrate is added as a 100  $\mu$ l argon-saturated solution. Ascorbate phenazine methosulfate (PMS) is added in the inhibited steady state. (B) CO (a 5 s bubbling) is added just before formate or during the steady state. ·····, control without CO.

without special techniques. This kinetics is slow in the presence of HQNO and can be separated into two phases (Fig. 6). The first is characterized by a  $t_{1/2}$  of 2–3 s, and corresponds to a decrease in the reduction level of approximately 50%. The second phase is slower ( $t_{1/2} = 12$  s) and produces reoxidation of 25% of the total level, giving a steady-state cytochrome *b* reduction level of approximately 25–30%. This result is consistent with at least two HQNO inhibition sites, one of which is located between cytochrome  $b_{NR}$  and the nitrate reductase.

The second reoxidation rate would indicate another site (rate limiting) located in the oxidase system or after the dehydrogenases. Note that only 40–50% of the first reoxidation phase could be recorded (Fig. 6).

#### *Cytochrome b reduction kinetics in the presence of NADH*

With NADH as donor, phase I is a real steady state (17%). It seems that in the presence of formate, the level increase is due to formate dehydrogenase activation as the oxygen disappears. The initiation of phase II corresponds to approximately 50  $\mu$ M of dissolved oxygen. The first-order constant for the phase II is lower with NADH (0.20  $s^{-1}$ ) than with formate (0.40  $s^{-1}$ ). But phases III and IV are difficult to distinguish. Transition from the oxidized state to the aerobic steady state occurs through a maximum.

Instead of getting the high steady-state level (65%) as in the case of formate with CO bubbling, the NADH addition first produces a 75–80% reduction increase, then an oscillatory decrease, until a steady state is reached (about 45% of total reduction).

In the presence of HQNO, cytochrome *b* reduction by NADH differs from formate reduction as the steady state is reached by a biphasic kinetics.

These results tend to support the general idea of a pathway common to formate and NADH-oxidase systems. However, the differences observed between formate and NADH may indicate the presence of a specific, but minor, NADH-oxidase pathway.

In the presence of menadione and NADH, cytochromes *b* reduction is much

more rapid than with only NADH. Rotenone decreases cytochromes reduction by NADH but is without effect when menadione is added. It agrees with the high nitrate reduction rate obtained with menadione and indicates that this artificial electron carrier is donating after rotenone site.

*Cytochrome b reduction kinetics in the presence of ascorbate phenazine methosulfate*

Upon addition of ascorbate phenazine methosulfate two cytochrome *b* reduction phases are observed (Fig. 7). First a steady state representing 30% of the final level, then a transition phase to anaerobicity exhibiting a synchronous reduction of cytochromes *b* and *d*. The two phases are characterized at room temperature by  $\alpha$  bands at 560 and 559 nm, respectively. It indicates that ascorbate phenazine methosulfate donates electrons close to cytochrome *b*-558. Although ascorbate phenazine methosulfate is autooxidizable, it is possible to measure a 50% inhibition of ascorbate phenazine methosulfate-oxidase system with 3 min of CO bubbling. In these conditions the steady state (45–50% of final cytochrome *b* reduction level) is obtained through a biphasic cytochrome *b* reduction curve.

HQNO increases the level of the aerobic steady state to approximately 50% (Fig. 7). It is characterized, as in the case without HQNO, by an  $\alpha$  band at 557.5 nm at liquid nitrogen temperature, while phase II of this reduction curve presents an absorption maximum at 556.5 nm. It can be deduced that HQNO does not modify the order of reduction of cytochromes *b* in the ascorbate phenazine methosulfate-oxidase system, and that a HQNO binding site is located between cytochrome *b*-558 and the terminal oxidase. Upon HQNO addition, the nitrate reduction steady-state level increases from 3% to 30% (Fig. 7). Keeping in mind that ascorbate phenazine methosulfate donates electrons close to *b*-558, this important change indicates an HQNO inhibition site between the cytochrome *b* associated to nitrate reductase and the nitrate reductase.

Ultraviolet irradiation produces a decrease in the aerobic steady-state level which would mean that a light-sensitive molecule may be the primary electron acceptor for ascorbate phenazine methosulfate.

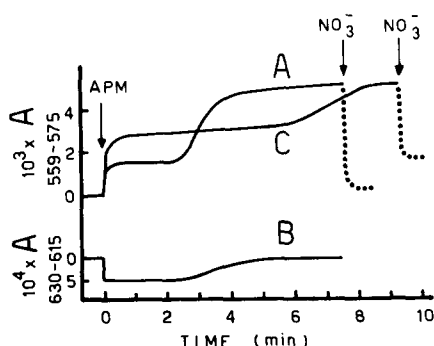


Fig. 7. Cytochromes *b* and *d* reduction by ascorbate phenazine methosulfate (curves A and B) and the effect of HQNO on cytochrome *b* reduction (curve C). HQNO (120  $\mu$ M) is added 5 min before ascorbate phenazine methosulfate (ascorbate  $2 \cdot 10^{-2}$  M; phenazine methosulfate  $5 \cdot 10^{-4}$  M). Nitrate ( $2 \cdot 10^{-2}$  M) is added as a 50  $\mu$ l argon-saturated solution. Vesicles 1.2 mg of protein/ml.

## Discussion

The respiratory system of anaerobically nitrate-grown *E. coli* cells contains the carriers necessary to reduce nitrate and oxygen at the expense of formate and NADH through an electron transfer segment common to all these systems. These results are consistent with a double-branched respiratory complex, as indicated in Scheme I.

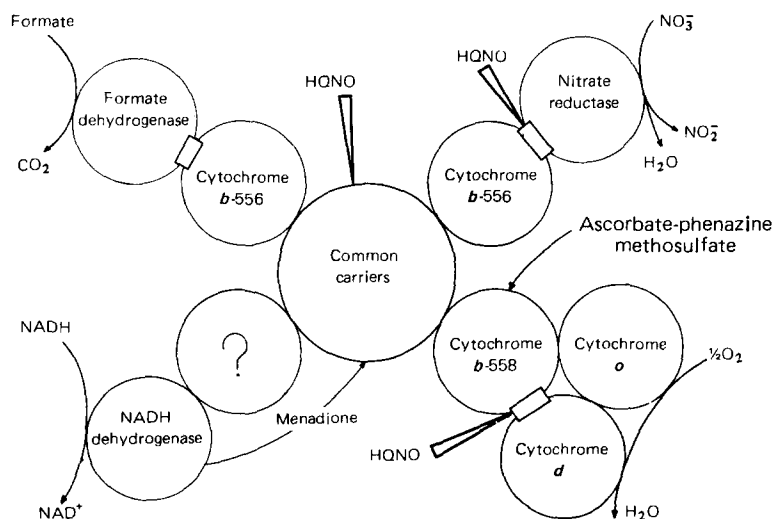
Four different *b*-type cytochromes are characterized in this work:

(i) The first *b*-type cytochrome is a very electronegative one which is not reduced at all by ascorbate phenazine methosulfate and only partially by NADH. This cytochrome may correspond to the already described formate dehydrogenase-associated cytochrome *b* [3]. It would be specific of anaerobic cells, since neither Bragg and Hou [11] nor Hendler et al. [12] report the presence of very electronegative cytochromes *b*.

(ii) The second is cytochrome *b*-558 which exists in anaerobic and aerobic cells [9,13]. Our results support the theory that this is the electron donor of cytochrome *d*. The cytochrome *b*-558 and cytochrome *d* concentration ratio is approximately 2.

(iii) The third is a *b*-type cytochrome located in a branch of the formate-oxidase system. On concentration (40% of the total 559 nm absorption) and spectral (*b*-556) grounds it is reasonable to attribute this *b*-type cytochrome to the nitrate reductase-specific system. This agrees with the purification of a nitrate reductase-bound cytochrome *b* [3]. This cytochrome would be inducible at the same time as nitrate reductase, and repressed by O<sub>2</sub>.

(iv) The fourth cytochrome is a CO binding cytochrome *b* with characteristics corresponding to the cytochrome *o* already described by Castor and Chance [8]. Another cytochrome, *b*-556, is generally described to be associated with cytochrome *o* [14], but we could not detect it.



Scheme I.

Two cytochromes may play the role of an oxidase in our membrane vesicles: cytochrome *o* and cytochrome *d* described by Pudek and Bragg in anaerobic cells of *E. coli* [13]. Cytochrome *d* appears as the only functional oxidase at high oxygen concentrations, while cytochrome *o* would operate only at very low partial oxygen pressure. This agrees with Haddock et al. [15], who did not find any cytochrome *b* competent for oxygen reduction in anaerobically nitrate-grown cells. Haddock's and Jones' conclusion [14] that cytochrome *d* would operate at lower oxygen concentrations than cytochrome *o*, does not seem to apply in the specific case of cells grown anaerobically with nitrate. In these cells there is, besides the nitrate system, at least one oxidase system, which makes the heterogeneity of cytochrome *b* less surprising. The association of a specific *b*-type cytochrome to initial and terminal enzymes seems to be a general phenomenon. It seems that the respiratory chain is the result of the association of these cytochrome *b*-enzyme complexes [3,16,17].

In Scheme I, a branching of the nitrate reductase system after cytochrome *b*-558 has been discarded by the breakdown of the respiratory complex by acetone/deoxycholate treatment (Forget, P., Sánchez A., unpublished results), which yields independent but functional cytochrome *b*-556 nitrate reductase and cytochrome *b*-558 oxidase complexes.

Scheme I presents evidence of three distinct sites of HQNO inhibition: one in each of the specific nitrate reductase and oxidase systems and a third, common to both systems. The arguments which are presented in favor of a common target to ultraviolet and HQNO [17] raise the possibility that quinones are present at different points in the respiratory complex. Chance's report [18] that both ubiquinone and naphthoquinone are present in *E. coli* respiratory chain supports this hypothesis.

### Acknowledgements

J.A.S.C. particularly thanks Dr. Sénez for his hospitality and assistance. The authors also thank Drs. P. Chevillote and Meunier for their interest and advice, and for making available the Aminco spectrophotometer used in this study. This work was supported by the grants c-36-75 and c-11 from Consejo de Desarrollo Científico y Humanístico, U.L.A., Mérida, Venezuela.

### References

- 1 Iida, D. and Taniguchi, R. (1959) *J. Biochem. Jap.* 46, 1041–1055
- 2 Ruiz-Herrera, J.A. and De Moss, J.A. (1969) *J. Bacteriol.* 99, 720–729
- 3 Enoch, H.G. and Lester, R.L. (1975) *J. Biol. Chem.* 250, 6693–6705
- 4 Corao, M.C., Serrano, J.A., Leal, J.A., Puig, J. and Muñoz, E. (1974) *Microbiol. Esp.* 27, 283–298
- 5 Lowry, O.H., Rosebrough, N., Farr, A.L. and Randall, R.J. (1951) *J. Biol. Chem.* 193, 265–275
- 6 Jones, C.W. and Redfearn, E.R. (1966) *Biochim. Biophys. Acta* 113, 467–481
- 7 Deeb, S.S. and Hager, L.P. (1964) *J. Biol. Chem.* 239, 1024–1031
- 8 Castor, L.N. and Chance, B. (1959) *J. Biol. Chem.* 234, 1587–1592
- 9 Shipp, W.S. (1972) *Arch. Biochem. Biophys.* 150, 459–472
- 10 Haddock, B.A. and Schairer, H.U. (1973) *Eur. J. Biochem.* 35, 34–45
- 11 Bragg, P.D. and Hou, C. (1967) *Arch. Biochem. Biophys.* 119, 194–208
- 12 Hendler, R.W., Towne, D.W. and Shrager (1975) *Biochim. Biophys. Acta* 376, 42–62
- 13 Pudek, M.R. and Bragg, P.D. (1974) *Arch. Biochem. Biophys.* 164, 682–693
- 14 Haddock, B.A. and Jones, C.W. (1977) *Bacteriol. Rev.* 41, 47–99
- 15 Haddock, B.A., Downie, J.A. and Garland, P.B. (1976) *Biochem. J.* 154, 285–294
- 16 Appleby, C.A. and Morton, R.K. (1954) *Nature* 173, 749–751
- 17 Cox, G.B., Newton, N.A., Gibson, F., Snoswell, A.M. and Hamilton, J.A. (1970) *Biochem. J.* 117, 551–562
- 18 Chance, B. (1955) *Faraday Discuss. Chem. Soc.* 20, 205–216